

Effect of Particle Size and Sand Inventory on Wall-to-Bed Heat transfer Characteristics of Circulating Fluidized Bed Riser

P. Mahanta, R.S. Patil, and M. Pandey

Abstract—The present paper describes a numerical study on the steady state wall-to-bed heat transfer characteristics of circulating fluidized bed (CFB) riser of cross section $0.15\text{ m} \times 0.15\text{ m}$ and height 2.85 (m) . 3-D CFD simulations for heat transfer characteristics were carried out for heated portion (heater) of 0.15 (m) width and 0.60 (m) height. Heater was placed 0.60 (m) above the distributor plate which is the lower splash region of CFB. For modeling and simulation, CFD code Fluent - version 6.3.26 has been used. Modeling and meshing were done with Gambit software – version 2.4.6. The wall of heater was maintained at the constant heat flux $q'' = 1000\text{ (W/m}^2\text{)}$. RNG $k\text{-}\epsilon$ model was used for turbulence modeling. Mixture model and Gidaspow model for phase interaction were used for the simulation of two phase flow (air + sand mixture flow) and Gidaspow model found to be more accurate model further simulations. Results obtained were compared for distribution of bed (air + sand mixture) temperature across the heater and local heat transfer coefficient along the height of the heater for two sand inventories (4 kg and 7 kg) and six particle sizes falling in the range of Geldart B type particles ($60\text{ }\mu\text{m}$, $100\text{ }\mu\text{m}$, $160\text{ }\mu\text{m}$, $260\text{ }\mu\text{m}$, $360\text{ }\mu\text{m}$, $460\text{ }\mu\text{m}$). Results obtained through CFD simulations were compared with available literatures and experimental results which were obtained from available CFB setup of IIT Guwahati.

Index Terms— Bed temperature, CFB riser, CFD simulations, Heat transfer coefficient.

I. INTRODUCTION

Recently use of circulating fluidized bed (CFB) boilers in power generation is gaining popularity because of its environmental compatibility and high efficiency. Circulating fluidized bed (CFB) is widely used for various industrial applications which include power generation, drying, cracking, and combustion. The increase and diversity in CFB applications demand the need for the development of more efficient experimental techniques, realistic simulations, and other research and design tools.

Versatile tool like CFD and related software's may be therefore used to accomplish the research with accuracy and also to overcome the limitations of experimental aspects. Some information on turbulence parameters which hard to

obtain in laboratory conditions which can be easily estimated using CFD tools [1], [2]. In addition, CFD models provide a more detailed data profile as a function of space and time without interfering or disturbing the flow by internal probes [1], [2].

Reference [3] has reported that dense flow hydrodynamic experiments measured either only the particle velocities or the particle concentrations until 1987. Studies on both the particle velocities, particle concentrations, which were determined together at first time for the riser flow by [4]. Since then, modelers been able to compare and evaluate their theoretical models with experimental studies in detail [1].

Reference [5] has reported that CFB riser involves dispersed gas-solid flow with very high velocity and strong interphase interactions. CFD simulation is a versatile tool to simulate two phase problems by predicting heat transfer characteristics such as temperature, heat transfer coefficient and hydrodynamic characteristics such as pressure, velocity, volume fraction etc.

Currently, the Eulerian–Eulerian (two-fluid) model with kinetic theory of granular flow is the most applicable approach to compute gas–solid flow in a CFB [6]–[8].

Reference [9] has reported that detailed discussion on the development of granular flow models.

Different drag models were used to predict the most representative gas–solid interphase exchange coefficient [10]–[12].

Reference [6] has used CFD tool to analyze gas solid flow. Gas / particle flow behavior in the riser section of a CFB, which was simulated using CFD package Fluent for velocity, volume fraction, pressure, and turbulence parameters for each phase. Reference [13] has developed a model using a Particle Based Approach (PBA) to accurately predict the axial pressure profile in CFBs. This simulation model also accounts for the axial and radial distribution of voidage and for the solids volume fraction.

Reference [14] has predicted the gas and solid velocity and volume fraction through 2-D simulation on CFB riser.

Reference [15] has done the simulations using Ansys CFX software version 10 and reported radial solid velocity profiles, computed on seven axial levels in the circular riser of a high-flux circulating fluidized bed (HFCFB) using a two phase 3-D computational fluid dynamics model.

Reference [16] has reported a multifluid Eulerian model integrating the kinetic theory for solid particles using Fluent-CFD software was capable of predicting the gas–solid behavior of a fluidized bed. Comparison of the model predictions, using the Syamlal–O'Brien, Gidaspow, and Wen–Yu drag functions, and experimental measurements on

Manuscript Submitted February 16, 2010.

P. Mahanta is with the Indian Institute of Technology, Guwahati, 781039 India (corresponding author, phone: +91 361 2583 126; fax: +91-361-2690762; e-mail: pinak@iitg.ernet.in).

R.S. Patil is with the Centre for Energy, Indian Institute of Technology, Guwahati, 781039 India (e-mail: patil@iitg.ernet.in).

M. Pandey is with the Mechanical Engineering Department, Indian Institute of Technology, Gandhinagar, 382424 India (e-mail: manmohan@iitgn.ac.in).

the time-average bed pressure drop, bed expansion, and qualitative gas–solid flow pattern indicated reasonable agreement for most operating conditions. Instantaneous and time-average local voidage profiles showed similarities between the model predictions and experimental results.

Reference [17] has reported a two-dimensional Eulerian–Eulerian model incorporating the kinetic theory of granular flow which was developed to describe the hydrodynamics of gas–solid flow in the riser section of a high density circulating fluidized bed. The predicted solid volume fraction and axial particle velocity were reasonably in good agreement with the experimental data. The developed model was capable of predicting the core-annular flow pattern and the cluster formation of the solid phase.

Reference [18] has reported that there will be erosion of the lower splash region during operation of CFB boiler, as lower splash region occupies dense hot stream of coal, limestone and sand etc. For designing the entire CFB, the study on lower splash region is therefore equally important as like study on the upper splash region.

Literature review reveals that many researches have reported CFD simulations based on only Eulerian model to predict only hydrodynamic characteristics for two phase flow in the CFB riser. Gas-solid flow can also be analyzed using other multiphase models such as mixture model and volume of fluid model. Therefore the present study is based on the CFD simulations by Fluent 6.3.26 [19] using Eulerian model as well as the mixture model, to predict heat transfer characteristics of air-sand flow in the lower splash region of CFB riser. Results obtained by the mixture model and Eulerian model with Gidaspow phase interaction scheme -drag model were compared for local heat transfer coefficient variation along the height of the heater and bed (air + sand mixture) temperature distribution across the heater. Also the effects of sand inventory and particle size on heat transfer characteristics were simulated and results obtained were compared with available experimental data and literatures.

II. EXPERIMENTAL SETUP

Figure 1 presents the CFB setup of 0.15 m × 0.15 m with a riser height of 2.85 m designed and fabricated at IIT Guwahati [20]. Riser of CFB setup was made up of plexiglass to facilitate flow visualization. A positive displacement type blower powered by a 20 HP motor supplies air. Figure 1 indicates: 1. Motor, 2. Blower, 3. Bypass valve, 4. Main control valve, 5. Water manometer, 6. Orifice plate, 7. Riser column, 8. Cyclone separator, 9. Downcomer, 10. Sand measuring section, 11. Butterfly valve, 12. Distributor plate, and 13. Heater section's positions, *U* (upper position), *M* (middle position) and *L* (lower splash region).

Experiments were conducted on the CFB unit with sand as the bed material and air as the fluidizing medium. Heat transfer characteristics along the riser were studied with incorporation of heater section in the lower splash region; having the same cross sectional area as that of the riser and height of 0.6 m.

The heater section was fabricated with MS sheet of 2 (mm) thickness with a height of 0.6 (m) as in Fig. 2. The constructional feature of the heater section as shown in Fig. 2 which includes: 1. Nichrome wire, 2. Mica, 3. Mica, 4. Thermocouple to measure heater's outer surface

temperature, 5. Asbestos sheet, 6. Ceramic wool, 7. MS wall, and 8. Bed thermocouples to measure the temperature along the height of the heater section.

Nichrome wire or heater coil of 2 (kW) capacities was wound over the mica sheet of 1.5 (mm) thickness which covers the MS wall of the heater section. Another mica sheet, which acts as an electric insulator, was wrapped over the Nichrome wire. To avoid the heat losses by radiation, ceramic wool and asbestos sheets were wrapped over the assembly. Heat was supplied to the heater section with electrical supply through an auto transformer.

To measure the temperature of the surface of the heater section and the bed, calibrated *T*- type thermocouples were installed in the same height on the wall as well as inside the heater section respectively as in Fig.3

Ten set of thermocouples with equal spacing of 5.5 (cm) along the height of the heater section were used to measure the bed temperature and surface temperature of the heater section, as in Fig. 3. A section *AA* was taken in the lateral direction at 0.16 (m) above the inlet of the heater and another one section was taken in the lateral direction 0.44 (m) above the inlet of the heater. Five thermocouples were placed along the

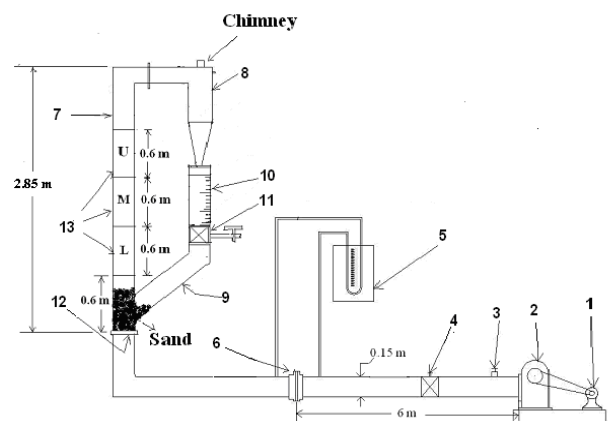


Fig. 1 CFB Setup

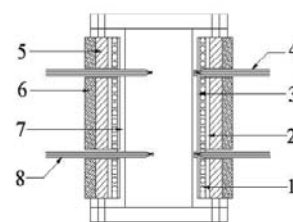


Fig. 2 Heater Section

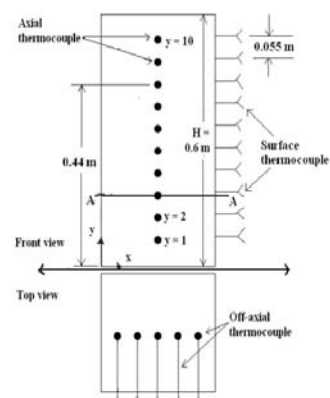


Fig. 3 Position of the Thermocouples

horizontal direction in these sections with equal spacing at the nondimensional distance $[X/b]$ of 0.1, 0.3, 0.5, 0.7 and 0.9, respectively as in Fig. 3.

Here the nondimensional distance $[X/b]$ is the distance X measured from the left hand side wall of the heater to the thermocouple end, normalized with respect to the width b of the heater.

III. EXPERIMENTAL HEAT TRANSFER STUDY

Steady state experiments were conducted on the CFB setup to examine the effect of bed cross section on heat transfer characteristics. Experiments were carried out for two sand inventories 4 (kg) and 7 (kg), superficial velocity 4 (m/s), particle size 460 (μm) and heat flux 1000 (W/m^2). Heat transfer experiments were also conducted using lower heat flux of 680 (W/m^2). In the present study, the results are presented only for heat flux of 1000 (W/m^2). This is because under the other similar operating conditions trends obtained for temperature profile, heat transfer coefficient and other type of graphs were similar for the heat flux $q'' = 680$ (W/m^2). Input heat flux q'' was restricted to 1000 (W/m^2) to prevent damage of plexiglass column of riser and to avoid breakage of Nichrome wire. Further, experiments were conducted with two different sand inventories (7 kg and 4 kg) so that weight per unit area of distributor plate P of each CFB setup was either 3050 (N/m^2) or 1750 (N/m^2). The range of the weight of sand inventory per unit area of the distributor plate 1750-3050 (N/m^2) was selected because beyond this limit of inventory, fast fluidization was not achievable. This is because there would be insufficient weight of sand inventory on the distributor plate to achieve fast fluidization if it was less than 1750 (N/m^2). Experiments could not be conducted for the value of P more than 3050 (N/m^2) because of constraint of maximum capacity of experimental setup (blower) to push the maximum weight of inventory of sand per unit area of distributor plate into the fast fluidization.

The local heat transfer coefficient h is calculated by

$$h = Q / [A_s \cdot (T_s - T_b)] \quad (\text{W} \cdot \text{m}^{-2} \cdot \text{K}^{-1}) \quad (1)$$

where Q is rate of heat supplied to the heater, measured using a Wattmeter. A_s is the surface area of heater, $q'' = Q/A_s$ is the heat flux, T type calibrated thermocouples and data acquisition system with Dasy Lab software version 8.0 was used to measure the surface temperature T_s and bulk mean bed temperature T_b . The local heat transfer coefficient is measured at 10 locations ($y = 1$ to 10 as in Fig. 3) along the height of heater.

Average heat transfer coefficient (h_{avg}) along the heater section at its any particular location above the distributor plate is calculated by

$$h_{avg} = \frac{1}{H} \int_0^H h_y \cdot dy \quad (\text{W} \cdot \text{m}^{-2} \cdot \text{K}^{-1}) \quad (2)$$

where H is the height of the heater (0.6 m), h_y is the local heat transfer coefficient. Local heat transfer coefficient (h_y) is

calculated at 10 different points ($y = 1, 2, \dots, 10$ as shown in Fig.3) along the height of heater section.

Uncertainty analysis was carried out for the heat transfer coefficient. Uncertainty is depending upon connections of thermocouples, accuracy of T type thermocouple ± 0.5 ($^\circ\text{C}$), wattmeter accuracy ± 5 (W), accuracy in length measurement ± 1 (mm) etc. Uncertainty analysis, using the method of Kline and McClintok [21], showed that the heat transfer coefficients estimated in the present study were within ± 4 %.

IV. CFD MODELING AND SIMULATION

In Fluent, the governing equations are discretized using the finite volume technique [22]. The discretized equations, along with the initial and boundary conditions, are solved to obtain a numerical solution. Mixture and Eulerian multiphase models were used for the simulation of air-sand flow. The parameters used for 3-D CFD simulations of heater section (portion L as in Fig.1) of cross section $0.15 \text{ m} \times 0.15 \text{ m}$ and height 0.6 (m) placed in the CFB riser of cross section $0.15 \text{ m} \times 0.15 \text{ m}$ and height 2.85 (m) as in Fig. 1

Density of sand = 2600 (kg/m^3), mean diameter of sand = 60- 460 (μm), density of air = 1.225 (kg/m^3), 3-D steady state solver, total number of tetrahedral cells = 40678 resulted from grid independence test for the CFB riser as Fig. 4, boundary conditions used as in Fig. 4 were air velocity inlet at bottom of riser = 4 (m/s), and volume fraction = 0; volume fraction of sand at inlet at right hand side wall of riser = 1 and sand velocity = 1.26 (kg/s); outlet boundary condition was pressure outlet at top of the riser = 0 (Pa) gauge pressure of air-sand mixture, turbulence model used = RNG k - ϵ model, numerical method used for pressure velocity coupling = phase coupled SIMPLE, discretization scheme = 1st order upwind, under relaxation parameters for pressure = 0.1, density = 0.1, body forces = 0.1, momentum = 0.1, volume fraction = 0.2, energy = 0.1; convergence criteria = 0.001, solution initialization = from all zones, length and width of the sand inventory = 0.15 (m) and height of the sand inventory in the CFB riser = 0.22 (m) and 0.13 (m) for 7 (kg) and 4 (kg) sand respectively during simulation.

In the Eulerian multiphase (gas-solid, two fluids) model, conservation equations of mass and momentum for both phases are developed and solved simultaneously. The link between the two phases is through the drag force in the momentum equations.

Continuity (k^{th} phase)

$$\frac{\partial}{\partial t} (\epsilon_k \rho_k) + \nabla \cdot (\epsilon_k \rho_k \vec{u}_k) = \sum_{p=1}^n \dot{m}_{pk} \quad (3)$$

where $k = f$ for fluid

$k = s$ for solids

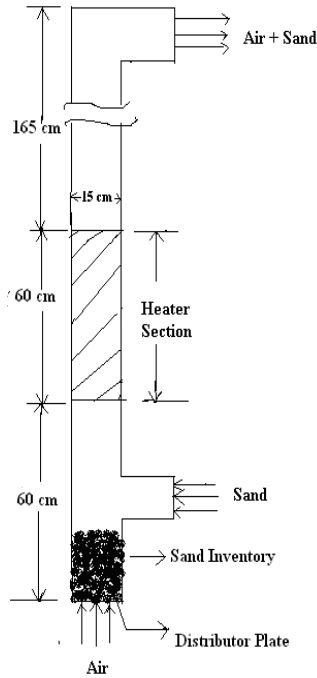


Fig. 4 CFB Riser

Momentum (fluid phase)

$$\frac{\partial}{\partial t}(\epsilon_f \rho_f \vec{u}_f) + \nabla \cdot (\epsilon_f \rho_f \vec{u}_f \otimes \vec{u}_f) = -\epsilon_f \nabla p + \nabla \cdot \vec{\tau}_f + \epsilon_f \rho_f \vec{g} + K_{sf}(\vec{u}_s - \vec{u}_f) + \vec{F}_f \quad (4)$$

Momentum (solids phase)

$$\frac{\partial}{\partial t}(\epsilon_s \rho_s \vec{u}_s) + \nabla \cdot (\epsilon_s \rho_s \vec{u}_s \otimes \vec{u}_s) = -\epsilon_s \nabla p - \nabla p_s + \nabla \cdot \vec{\tau}_s + \epsilon_s \rho_s \vec{g} + K_{sf}(\vec{u}_f - \vec{u}_s) + \vec{F}_s \quad (5)$$

Total volume fraction conservation

$$\epsilon_s + \epsilon_f = 1 \quad (6)$$

Equation (3) represents the mass balance of each phase with temporal and spatial gradients on the left hand side and mass creation (\dot{m}) of the p_{th} species (in this case, zero) by reaction or phase change. Equations (4) and (5) are momentum conservation equations for the fluid (air in this case) and solid phase, respectively. The left side represents temporal and spatial transport terms whereas the right hand side has terms for the various interaction forces involved. Note that the hydrodynamic pressure is shared by both phases and hence, the gradient of pressure (p) is premultiplied by the respective volume fractions (ϵ) in both equations. (ρ), (\vec{u}) and (\vec{g}) represent to density, velocity and acceleration due to gravity respectively. The stress term (τ_f) represents the shear stress in gas phase in (4). Equation (5) represents the solids phase equation, where (τ_s) represents the shear stress term due to collision among particles.

Terms $K_{sf}(\vec{u}_f - \vec{u}_s)$ and $K_{sf}(\vec{u}_s - \vec{u}_f)$ represent the momentum exchange or

drag between the two phases in (4) and (5). These terms are equal in magnitude and opposite in sign and account for the friction at the interface between the phases. The terms (\vec{F}_f) in (4) and (\vec{F}_s) in (5) represent all other forces that may affect the flow, such as electrical, magnetic and other effects.

The drag is an effective way of representing the surface integral of all the forces that exist at the interface between the phases. Interphase momentum exchange factor of Gidaspow's drag closure as in (7).

For

$$\epsilon_g > 0.8,$$

$$K_{s,f} = \frac{3\epsilon_s \epsilon_g \rho_g}{4d_s} C_{d,s} (\epsilon_g^{-2.65}) |\vec{u}_s - \vec{u}_g| \quad (7)$$

$$C_{d,s} = \frac{24}{\epsilon_g \cdot Re_s} [1 + 0.15 \cdot (\epsilon_g \cdot Re_s)^{0.687}]$$

For

$$\epsilon_g \leq 0.8,$$

$$K_{s,f} = 150 \cdot \frac{\epsilon_s^2 \cdot \mu_g}{\epsilon_g \cdot d_s^2} + 1.75 \cdot \frac{\epsilon_s \cdot \rho_g}{d_s} |\vec{u}_s - \vec{u}_g|$$

where Re_s and d_s are the Reynolds number and diameter of solid particles respectively and other symbols have their standard meaning which already are defined.

In the mixture (homogeneous) model, it is assumed that both phases are having the same velocity and no slip condition was applied to simulate the flow. The mixture model does modeling for two phases (fluid or particulate) by solving the momentum, continuity, and energy equations for the mixture, the volume fraction equations for the secondary phases, and algebraic expressions for the relative velocities.

Entire CFB riser was modeled and meshed in Gambit. Tetrahedral cells of 40678 were selected for its simulation. Energy equation (8) was applied during heat transfer 3-D simulations for heater section as in Fig.4.

$$\frac{\partial}{\partial t}(\rho E) + \nabla \cdot (\vec{v}(\rho E + p)) = \nabla \cdot (k_{eff} \nabla T - \sum_j h_j j_j + \vec{\tau}_{eff} \cdot \vec{v}) + S_{hj} \quad (8)$$

where effective conductivity (k_{eff}) and is the diffusion flux (j_j) of species j .

The four terms of the right hand side in (8) represents energy transfer due to conduction, species diffusion, viscous dissipation and volumetric heat sources (S_{hj}).

Now, heat transfer simulations (by enabling energy equation) for the heater section were carried out using both multiphase models to obtain the bulk mean bed temperature (T_b) and wall temperature (T_s). Simulations were carried at constant heat flux $q'' = 1000$ (W/m²) for different sand inventory and particle size for a superficial velocity of 4 (m/s). Local convective heat transfer coefficient h is calculated by using (1). Simulated results were compared with experimental results. Results and discussion is explained in the following section.

V. RESULTS AND DISCUSSION

A. Studies on Multiphase Model Comparison

Different multiphase models - Eulerian model and mixture model (homogeneous model) available in Fluent were used to simulate the two phase flow. Phase interaction model -Gidaspow scheme is used for the phase interaction. Bed temperature distribution any section across the width of the heater and surface temperature of the wall were obtained after the convergence of code. Equation (1) is used to determine local heat transfer coefficient. Numerical experiments were conducted at superficial velocity 4 (m/s), bed inventory 7 (kg), heat flux 1000 (W/m²) and particle size 460 (μm).

Figure 5 shows that the variation of local heat transfer coefficient along the height of the heater. Trends and values of heat transfer coefficient show that the trends and values obtained by Eulerian model with Gidaspow phase interaction scheme are more close to that of experimental values than multiphase mixture model. The values obtained by mixture model were considerably away from experimental values. Therefore in the further study the Eulerian model with Gidaspow phase interaction scheme is selected to study the effect of inventory and particle size on heat transfer characteristics rather than multiphase mixture model.

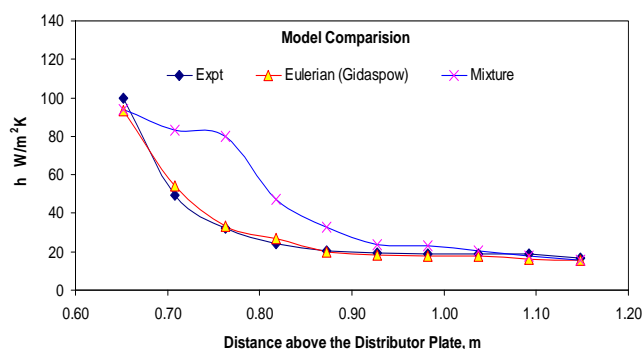


Fig. 5 Heat Transfer Coefficient Distribution

B. Studies on Effect of Sand Inventory on Heat Transfer Characteristics

Figures 6-8 show the effect of bed inventory on the distribution of bed temperature and heat transfer coefficient. Eulerian multiphase model with Gidaspow phase interaction scheme was used to simulate the two phase flow. Inventory in the bed was varied from 4 (kg) to 7 (kg). Parameters velocity 4 (m/s), heat flux 1000 (W/m²) and particle size 460 (μm) were maintained same for the simulations conducted for the different inventories. It is observed that increase in the inventory of sand in the riser increases the bed temperature and heat transfer coefficient. This is because sand particles concentration increases with increase inventory of the bed. Consequently, more quantity of particles in the lower splash region promotes more heat transfer through conduction, because of which bulk temperature of bed across the sections taken at 1.04 (m) and 0.76 (m) above the distributor plate was observed to be higher than that for the lower inventory.

C. Studies on Effect of Particle Size on Heat Transfer Characteristics

Effect of particle size on heat transfer characteristics was completed for the Geldart B Type of the particles. The

experiments on CFB setup and Fluent were using particles of average size of 460 (μm). Results obtained were in good agreement as in Fig. 9. Now using only Fluent, it was more convenient to study the effect of other particles with average size of 60 (μm), 100 (μm), 160 (μm), 260 (μm), 360 (μm) on the heat transfer characteristics. Eulerian multiphase model with Gidaspow phase interaction scheme was used to simulate the two phase flow. Simulations were conducted on different particle sizes at the same bed inventory- 7 (kg) of sand and same superficial velocity of air 4 (m/s). Also, wall of the heater section was with constant heat flux 1000 (W/m²), it was observed that heat transfer coefficient increase with increase in particle size as shown in Figs. 9-10. Local and average heat transfer coefficient was calculated as in (1) and (2) respectively. The physics or reason behind this was the effective erosion of boundary layer around the heater surface which results in decrease the heat transfer resistance in the beds of relatively larger particles, with a consequent increase in heat transfer with increasing particle size. The trends obtained were similar to results reported in literature [23], [24].

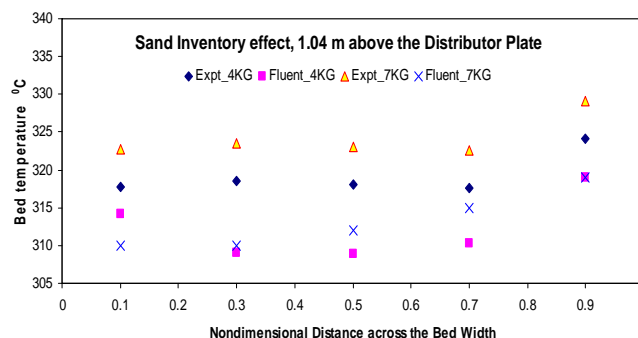


Fig. 6 Bed Temperature Distribution

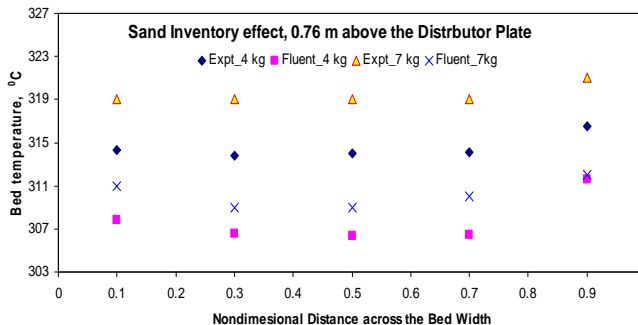


Fig. 7 Bed Temperature Distribution

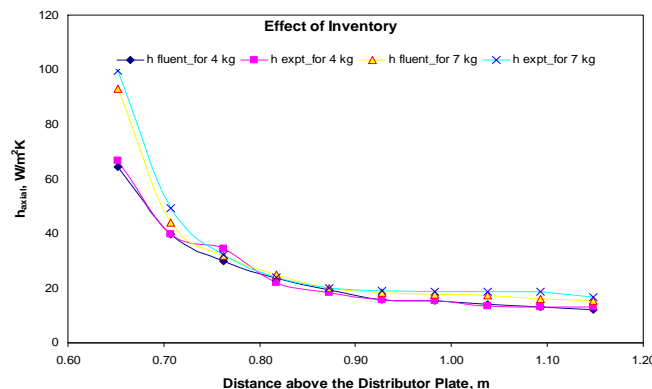


Fig. 8 Heat Transfer Coefficient Distribution

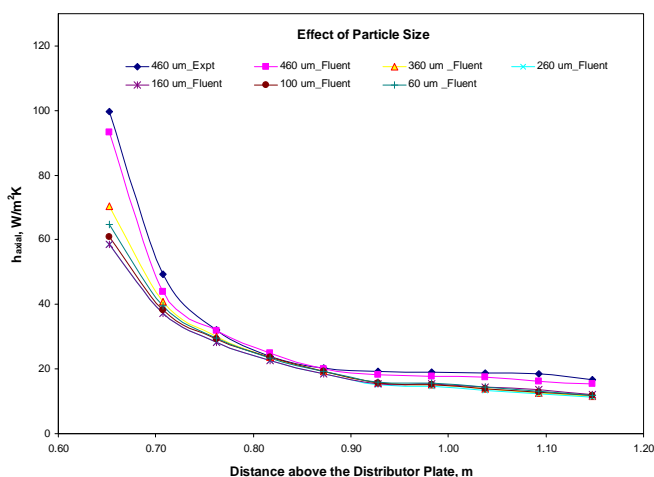


Fig. 9 Local Heat Transfer Coefficient Distribution

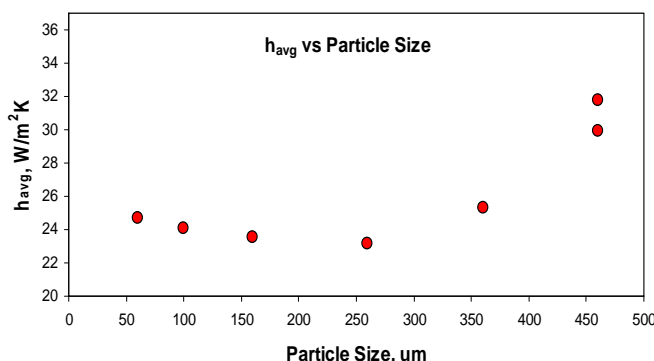


Fig. 10 Average Heat Transfer Coefficient Distribution

VI. CONCLUSIONS

Heat transfer experiments were conducted on in-house fabricated CFB setup – at the bottom region (denser region of sand particles) via heater, and 3-D numerical simulations using Fluent. Numerical and experimental results were in good agreement. Eulerian-Eulerian multiphase model with Gidaspow phase interaction scheme is found to be more accurate model to simulate the two phase flow rather than mixture model. Effect of sand inventory and particle size on heat transfer characteristics was studied. Bed temperature and heat transfer coefficient increases with increase in bed inventory and particle size.

REFERENCES

- [1] A. Almuttahir and F. Taghipour, "Computational fluid dynamics of high density circulating fluidized bed riser: Study of modeling parameters", *Powder Technol.*, vol. 185, 2008, pp.11–23.
- [2] V. Ranade, *Computational flow modeling for chemical reactor engineering*, Acad. Press, 2002. pp. 19–20.
- [3] A. Miller, D. Gidaspow, "Dense, vertical gas–solid flow in a pipe", *AIChE J.*, vol. 38, 1992, pp.1801–1814.
- [4] R. Bader, J. Findlay, T. Knowlton, "Gas/solid flow patterns in a 30.5-cm diameter circulating fluidized bed", in: *P. Basu, J. Large (Eds.), Circulating Fluidized bed Technology II*, Pergamon Press, 1988.

- [5] R.S. Patil, M. Pandey and P. Mahanta, "CFD simulations for heat transfer and hydrodynamic characteristics of circulating fluidized bed riser", *1st International Conference on Energy Engineering and Eco-Balance (IC-EEE)*, MITR Pune, India, 16-18th Feb., 2009.
- [6] S. Benyahia, H. Arastoopour, T. Knowlton, H. Massah, "Simulation of particles and gas flow behavior in the riser section of a circulating fluidized bed using the kinetic theory approach for the particulate phase", *Powder Technol.*, vol. 112, 2000, pp. 24–33.
- [7] C. Chan, Y. Guo, K. Lau, "Numerical modeling of gas–particle flow using a comprehensive kinetic theory with turbulent modulation", *Powder Technol.* vol.150, 2005, pp. 42–55.
- [8] Y. Zheng, X. Wan, Z. Qian, F. Wei, Y. Jin, "Numerical simulation of the gas–particle turbulent flow in risers reactor based on $k-\epsilon-k_p-\epsilon_p-\Theta$ two fluid model", *Chem. Eng. Sci.* vol. 56, 2001, pp. 6813–6822.
- [9] D. Gidaspow, *Multiphase flow and fluidization: continuum and kinetic theory description*, Academic Press, Boston, 1994.
- [10] D.Gidaspow, R.Bezburuah, J.Ding, "Hydrodynamics of circulating fluidized beds, kinetic theory approach", *Fluidization VII, Proceedings of the 7th Engineering Foundation Conference on Fluidization*, 1992, pp. 75–82.
- [11] H. Arastoopour, P. Pakdel, M. Adewumi, "Hydrodynamic analysis of dilute gas–solids flow in a vertical pipe", *Powder Technol.*, vol. 62, 1990, pp. 163–170.
- [12] M. Syamlal, T. O. Brien, *Derivation of a drag coefficient from velocity-voidage correlation*, U.S. Dept. of Energy, Office of Fossil Energy, National Energy Technology Laboratory, Morgantown, West Virginia, April, 1987.
- [13] A. Gungor, "Predicting axial pressure profile of a CFB", *Chem. Eng. Sci.*, vol. 140, 2008, pp. 448-456.
- [14] A. Almuttahir and F. Taghipour, "Computational fluid dynamics of a circulating fluidized bed under various fluidization conditions", *Powder Technol.*, vol. 63, 2008, pp. 1696-1709.
- [15] J.C.S.C. Bastos, L.M. Rosa, M. Mori, F. Marini, and W.P. Martignoni, "Modelling and simulation of a gas–solids dispersion flow in a high flux circulating fluidized bed (HFCFB) riser", *Catalysis Today*, vol. 130, 2008, pp. 462-470.
- [16] F.Taghipour, N.Ellis and C. Wong, "Experimental and computational study of gas–solid fluidized bed hydrodynamics", *Chem. Eng. Sc.*, vol. 60, 2005, pp. 6857 – 6867.
- [17] A. Almuttahir and F. Taghipour, "Computational fluid dynamics of a circulating fluidized bed under various fluidization conditions", *Chem. Eng. Sc.*, vol. 63, 2008, pp. 1696 – 1709.
- [18] R.S Patil, M. Pandey, P. Mahanta, "Study on the heat transfer characteristics in the lower splash region of circulating fluidized bed riser", *7th World Conference on Experimental Heat Transfer, Fluid Mechanics and Thermodynamics (ExHFT-7)*, Krakow, Poland, 2009, pp. 555.
- [19] Fluent 6.3.26 Manual
- [20] M.Pandey, P. Mahanta, R.S. Patil, M.V. Gawali, "Development of an experimental facility for the study of scale effects in circulating fluidized beds", *National Conference on Recent Advances in Mechanical Engineering (NCRAME)*, Silchar, India, 2008, pp.170-175.
- [21] S.J.Kline, F.A. Mcclintok, "Describing uncertainties in single – sample experiments", *Mech. Eng.* 1953, pp. 3.
- [22] S. Patankar, *Numerical Heat Transfer and Fluid Flow*, Hemisphere, Washington, DC, 1980.
- [23] G.R. Grulovic, N.B. Vragolovic, Z. Grbavcic, Z. Arsenijevic, "Wall-to-bed heat transfer in vertical hydraulic transport and in particulate fluidized beds", *Int. J. Heat Mass Trans.*, vol. 51, 2008, pp. 5942-5948.
- [24] S.D. Kim, J.S. Kim, C.H. Nam, S.H. Kim, Y. Kang, "Immersed heater-to-bed heat transfer in liquid–liquid–solid fluidized beds", *Chem. Eng. Sci.*, vol. 54 (21), 1999, pp.5173–5179.